Interindividual Differences in Functional Interactions among Prefrontal, Parietal and Parahippocampal Regions during Working Memory

Michael F. Glabus[1,2], Barry Horwitz[3], John L. Holt[1,2], Philip D. Kohn[1,2], Brooke K. Gerton[1,2], Joseph H. Callicott[2], Andreas Meyer-Lindenberg[1,2] and Karen Faith Berman[1,2]

[1]Unit on Integrative Neuroimaging, National Institutes of Health, Department of Health and Human Services, 9000 Rockville Pike, Bethesda, MD, 20892-1365, USA, [2]National Institute of Mental Health, National Institutes of Health, Department of Health and Human Services, 9000 Rockville Pike, Bethesda, MD, 20892-1365, USA and [3]Brain Imaging and Modeling Section, National Institute on Deafness and other Communication Disorders, National Institutes of Health, Department of Health and Human Services, 9000 Rockville Pike, Bethesda, MD, 20892-1365, USA

To clarify the neural systems deployed by individual subjects during working memory (WM), we collected functional neuroimaging data from healthy subjects, and constructed a model of 2-back WM using structural equation modeling (SEM). A group model was constructed, and models for each subject were validated against it. The group model consisted principally of regions in the prefrontal and parietal cortex, with considerable interindividual variance in the single-subject models. To explore this variance, subjects were split into two groups based on performance. Performance level and self-reported strategy scores were used in a correlation analysis against path weights between nodes of individual models. High performers utilized a left hemisphere sub-network involving inferior parietal lobule and Broca's area, whereas lower performers utilized a right hemisphere sub-network with interactions between inferior parietal lobule and dorsolateral prefrontal cortex. Further, we observed an interaction between the parahippocampal formation and the inferior parietal lobule that was related to the different strategies used by the individuals to perform the task. Strategy and performance level appear to be intricately related in this task, with neural systems supporting verbal processing producing better performance than those associated with spatial processing. These results demonstrate that individual behavioral characteristics are reflected in specific neurofunctional patterns at the system level and that these can be captured by analytical techniques such as SEM.

Introduction

It has become increasingly apparent that all but the simplest functions require coordinated activity among networks of brain regions, rather than depending upon a single, segregated region, and that there are likely to be interindividual differences in the way humans bring these networks to bear on cognitive tasks. Studies in nonhuman primates have provided important evidence that the neural substrate supporting working memory (WM) is no exception to the first of these assertions, and that prefrontal cortex and parietal regions have particular primacy in this system (Friedman and Goldman-Rakic, 1994; Chafee and Goldman-Rakic, 1998). Functional neuroimaging has identified these regions as co-activated in groups of humans performing WM tasks (Hartley and Speer, 2000), in accord with the proposal that the WM central executive is supported by phonological and visuospatial rehearsal systems (Baddeley, 1992). The now extensive WM neuroimaging literature at the group-average level suggests that the supporting system is more extensive, encompassing not only dorsolateral prefrontal and parietal regions, but premotor, anterior cingulate cortex, Broca's area, and cerebellum as well (Smith and Jonides, 1998, 1999; Cabeza and Nyberg, 2000).

Functional neuroimaging has begun to provide clues about the workings of separate neural components of this WM system in individuals (Rypma and D'Esposito, 1999). However, there has been little formal analysis of interregional interactions in single subjects, particularly in the domain of WM. Thus, it is not clear how these regions dynamically interact in individuals or how individual differences in subject performance or strategy are reflected in these system-level networks. Understanding how self-reported strategy is reflected at the system level would clarify the role of distinct networks of brain regions in cognition. Identifying individual characteristics in brain network interactions has clear import for understanding differences in abilities and cognitive styles among healthy subjects and holds great promise for elucidating the neurobiology of learning (Buchel *et al.*, 1999) and of abnormal cognition in psychiatric and neurological patients.

Covariance-based methods that assess the within-task, interregional effective connectivity in activated brain networks can be implemented using structural equation modeling (SEM) (McIntosh and Gonzalez-Lima, 1994; McIntosh *et al.*, 1996a; Buchel and Friston, 1997). SEM belongs to a class of multivariate modeling methods that includes eigenimage and partial least-squares (PLS) analysis. SEM applied to neuroimaging examines the covariance matrix between tasks within-group or between groups, within-task. Eigenimage analysis allows the specification of temporally-dependent brain activation patterns of functional connectivity between conditions or groups of subjects, where each eigenvector is associated with a unique pattern of brain activation (Friston, 1994). PLS is similar to eigenimage analysis in that it uses single-value decomposition to model patterns of activation but includes experimental design, block effects, and behavioral outcomes (McIntosh *et al.*, 1996b). SEM differs fundamentally from the other two methods in that it attempts to identify the explicit influence of one brain region on another (Horwitz *et al.*, 1999). These models are usually constrained by known anatomical connections within the network, along with identification of the regional pattern of activation. In PET and fMRI this typically means an increase in signal that reflects synaptic processes (Waldvogel *et al.*, 2000; Logothetis *et al.*, 2001). Most models are derived at the group-average level, with a single cohort tested across a number of experimental conditions (McIntosh *et al.*, 1996a), or multiple groups across one experimental condition (Horwitz *et al.*, 1995).

Cerebral Cortex December 2003;13:1352–1361; DOI: 10.1093/cercor/bhg082

The aim of the current study was to use SEM with PET data acquired during a WM task (Callicott *et al.*, 1999) that allows different strategies for successful performance, and to assess how strategy and performance level are reflected in the functional networks, both for the group as a whole, and in *individual* subjects. We were particularly interested in gaining knowledge on how well different self-reported cognitive strategies can be discriminated at the cortical level. Our hypotheses, based on previous work, were that we would see different networks of activity in different hemispheres reflecting spatial or verbal strategies (Smith and Jonides, 1998; Gevins and Smith, 2000), and that collaborative activity between frontal and parietal regions would reflect a given subject's task performance (Diwadkar *et al.*, 2000).

Materials and Methods

Subjects

Data were collected from a group of 39 healthy right-handed control subjects consisting of 17 females and 22 males with a mean age of 30 years (range 20–48). Subjects were fully informed and gave written consent to participate in accordance with the study protocol approved by the NIMH Institutional Review Board and the NIH Radiation Safety Committee. Prior to scanning, all subjects were trained until they reached a consistent level of performance.

Experimental Task and Data Acquisition Procedures

The WM task was an adaptation of the *n*-back task designed for use in EEG studies (Gevins and Cutillo, 1993) and utilized with neuroimaging (Weinberger *et al.*, 1996; Callicott *et al.*, 1998). Briefly, subjects are presented with a diamond-shaped figure containing four circles, one in each corner (Fig. 1, left panel). A single number (1, 2, 3 or 4) appears at random in one of the four positions, but the same number (e.g. 2) always appears at the same spatial location (i.e. left circle). Stimuli are presented for 1.5 s and each trial lasts for 2 s. Subjects are asked to remember the current number and to press one of four buttons, using their right thumb, on a diamond-shaped button box. In this task, the subject must make a response at every stimulus presentation. For the 0-back condition, the subject maps the current number to the position on the button box, while for the 2-back condition the subject maps the stimulus presented two-before to the appropriate button on the box. Thus, the 2-back condition contains a WM and a sensorimotor element, whereas the 0-back condition contains only a sensorimotor element (notwithstanding having to keep the basic task requirements in mind). In the WM condition the encoding, maintenance and retrieval processes occur concurrently and with every stimulus presentation, and thus they cannot be separated into discrete components with the paradigm used.

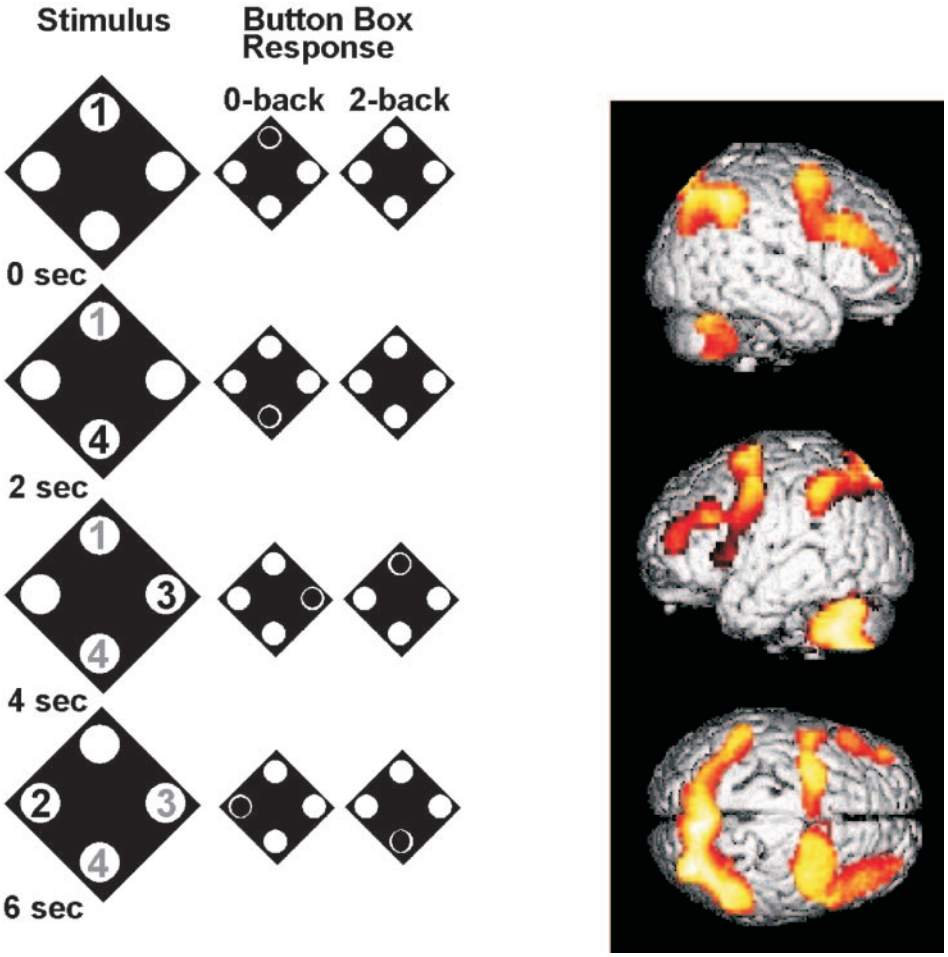

Figure 1. Left panel: the n-back WM task. A number is presented at random in the corner of the diamond-shaped figure (left) (the stimuli are presented every 2 s, for 1.5 s duration). The subject maps their response on to a diamond-shaped button box (right). For the 2-back response, the subject responds by pressing the button that corresponds to the stimulus presented two-before the current stimulus. The black number represents the current stimulus, the gray numbers those currently being held in WM and are shown for illustration purposes only — the subject would only see the black number. Right panel: SPM96 map showing the brain regions that activate in the 2-back task compared with the 0-back task. The statistical threshold is set to display Z-values greater than 4, corrected for multiple comparisons. Activation sites and coordinates are listed in the Table 1.

It is possible for subjects to use a spatial strategy (remembering the spatial positions of the presented numbers), a verbal strategy (subvocally rehearsing the presented numbers), or a combination of both to perform this task. Data were collected from 14 of the 39 subjects on cognitive strategy (spatial or verbal) via a five-point scale that classified task strategy in verbal:spatial percentage ratios, where 1 = 100:0, 2 = 75:25, 3 = 50:50, 4 = 25:75, 5 = 0:100.

Imaging data were acquired while subjects lay supine in a GE Advance, 3D PET camera (GE Medical Systems, Milwaukee, WI) using an i.v. bolus of 10 mCi of $H_2{}^{15}O$ for each scan. Head position was maintained using a thermoplastic face-mask. Twenty-six subjects had 14 0-back alternating with 14 2-back scans collected in two separate sessions spread over 2 days with no more than 2 weeks between sessions. Thirteen subjects had only seven 0-back and seven 2-back scans. The scans occurred at 6 min intervals and PET data were collected for 60 s during 2 min of stimulus presentation, allowing 61 trials. Each subject's performance was logged on a laptop computer that recorded responses to each stimulus.

Image Data Processing

PET images were converted to Analyze format (Biomedical Imaging Resource, Mayo Clinic, Rochester, MN). Data for each subject were motion-corrected using AIR 3.0 (Woods *et al.*, 1992). A mean image was made from all co-registered 2-back and 0-back scans. Images were then processed and analyzed with SPM96 (Friston *et al.*, 1995) as follows: the mean image was spatially normalized against a PET brain template image supplied with the software. The normalization process used linear (12-point Affine) and non-linear (Basis functions: '4, 5, 4') options. The computed spatial normalization parameters for each subject's mean-image were then applied to their 0-back and 2-back images. Voxel dimensions after normalization were $2 \times 2 \times 4$ mm in the x, y and z dimensions, respectively. All normalized images were subsequently smoothed with a Gaussian kernel (10 mm FWHM, isotropic) to reduce noise and interindividual differences in gyral and sulcal anatomy. The data were then analyzed using the PET statistics toolbox in SPM96, first being proportionally scaled to the global mean intensity across all scans for all subjects, then analyzed using a 'multiple-subject replication of conditions' design. Two contrasts were produced: (i) showing increases in the 2-back versus the 0-back condition; (ii) showing reductions in the 2-back versus 0-back condition.

SEM Methods

The method we adopted to construct our SEM models was based on published methodology (McIntosh and Gonzalez-Lima, 1994; Goncalves *et al.*, 2001). Briefly, this involved combining anatomical and functional information to help define brain nodes and interregional connections. A correlation matrix was derived from the regional intensities of the 2-back activation scans. The observed correlation matrix was tested against an expected correlation matrix, generated by the SEM software, and the validity of the model was established using stability and fit criteria (defined below). One half of the data were tested against the other half (see below, the split-half method), as no accepted model existed to test the complete data set against. Once a stable, unique and good-fitting group model was established, individual models for each subject were constructed in a similar manner, then tested against the group model using the same indices of stability and fit. The specific details of how this was achieved are now given.

The Group WM Model

Data Extraction: Regions of Interest and Coordinates

The coordinates of the brain regions included in the model were derived by examining in detail the group contrast-of-conditions output from SPM for the 2-back task versus the 0-back task. Coordinates of the principal sites of activation were determined and used as a guide for extracting information from individual subjects images. The group analysis represents the average location of the sites of activation for all the subjects. An algorithm was used to extract the average count data in a region, 5 by 5 by three voxels in the x, y and z dimensions, centered on the selected voxel — a volume of 1.2 cm^3 ($10 \times 10 \times 12$ mm) — for each subject.

Constructing the Group Model

The group network model of WM was constructed guided by regions activated during the 2-back WM task. The process involved two stages: identifying the anatomical nodes and the functional connections between them; establishing the directionality of the connections between the nodes during the modeling process.

The model was based on known anatomical connections in human and non-human primates (Middleton and Strick, 1994, 2000, 2001; Petrides and Pandya, 1999; Clower *et al.*, 2001) and on data from published functional imaging studies (Kim *et al.*, 1994; Andreasen *et al.*, 1998). Paths between some regions without known direct anatomical connections, but which have documented functional interactions, were also included (McIntosh and Gonzalez-Lima, 1994). Using putative connections based on function is acceptable in modeling higher order cognitive processes, essentially accounting for interactions mediated by regions not in the model.

Extracted regional activity was averaged across all scans for the 2-back condition for each of the 39 subjects at each node, and a group interregional correlation matrix was produced. A group SEM WM model was constructed from the group correlation matrix using the MX (Neale *et al.*, 1999) SEM software (supplied by Dr Michael Neale, Virginia Commonwealth University, http://views.vcu.edu/mx/). The standard approach was adopted: to construct a group WM model based on all the data, then to test the expected correlation matrix generated by the model against the experimentally observed correlation matrix. The presence and directionality of paths were established using a combination of *a priori* information and information obtained during the modeling process. It should be noted that these paths represent *functional connections during the WM process* and not the anatomical connections *per se*.

Testing the Group Model

The steps in WM model construction involved testing the validity of path connections with indices of stability and fit, then adjusting the residual variance, Psi (Ψ), downwards and re-testing the model in an iterative manner. Ψ is a measure of the proportion of the total variance due to the combined influence of regions outside the model, and is included as a residual term in the model (Bullmore *et al.*, 2000). The value that Ψ is set to specifies the amount of residual variance that is used in the model (McIntosh and Gonzalez-Lima, 1994; Goncalves *et al.*, 2001). Setting the value of Ψ has been fairly arbitrary in PET studies in the past, but fixing its value reduces the number of model parameters that must be estimated, leading to more stable models. However, the higher Ψ is set, the less variance the model has to work with and the more unlikely that a unique solution will be found, while freeing the parameter completely can lead to model indeterminacy. The lowest possible value of Ψ, while maintaining model stability, is the aim. The method for determining the 'best' Ψ for the model is a balance between ensuring the model is a good fit and that the solution is fairly unique.

Thus, once a stable model was found with Ψ set to an initial value of 0.7, it was incrementally reduced and the model re-tested, using two goodness-of-fit indices: the Akaike Information Criteria (AIC) (Akaike, 1987) and the root-mean-square error of approximation (RMSEA) (Browne and Cudeck, 1993). The rule-of-thumb for assessing goodness-of-fit is that a zero or negative AIC and RMSEA value of ≤ 0.1 are desirable (Neale *et al.*, 1999). Paths were initially modeled between nodes, individually in one of two directions, then together in both directions at the same time. The most parsimonious fit, derived from the goodness-of-fit indices, was used to determine path inclusion. This method is equivalent to bootstrapping the model prior to the next stage, and adjusting the residual variances. In summary, our approach was to define a model, then to test it and a series of close alternatives using goodness-of-fit indices to establish that our proposed model was amongst the best-suited for describing the functional interactions implicit to our data set (Bullmore *et al.*, 2000).

The Split-half Method

The group WM model was tested using the split-half method (McIntosh and Gonzalez-Lima, 1994). Because there was no clearly established model against which to test our proposed model, we adopted a conservative approach where we construct a model on one half of the data and test it on the other half. The method uses a stacked-model configuration,

where null and alternative models are compared. In one half of the stack (the null) equivalent SEM paths across models are constrained to be the same and the χ^2 statistic is computed. In the second half of the stack (the alternative) the equivalent paths across the two models are freed and the χ^2 statistic is again computed. The *P*-value is established by referring to a χ^2 table, employing the difference in degrees-of-freedom between null and alternative models.

The two sub-groups were matched for age, sex and performance. Null and alternative models were assessed for fit using the χ^2 difference between null and alternative models. Residual variances on model nodes were lowered from 0.7 until a *P*-value for the χ^2 difference statistic was >0.1. Lowering the Ψ allows the model more freedom to fit individual paths, providing the fit is stable. A probability value greater than 0.1 indicates that, under the null-hypothesis, there is no significant difference between the observed and expected interregional correlation matrices, and thus the model fit is acceptable, by conventional standards (Bullmore *et al.*, 2000), providing the AIC indicates a stable model.

Single-subject WM Models

Data Extraction: Regions of Interest and Coordinates

To account for interindividual differences in 2-back WM activation patterns, 39 'single-subject replication of conditions' designs were performed on the 2-back versus 0-back scans, one for each subject. Coordinates for the principal sites of activation for each subject were then determined from these analyses and used as a guide for extracting the proportionally scaled intensity values from each individual's 2-back scans. The loci of activation for individual subjects were defined within one FWHM (10 mm isotropic) of the spatial smoothing filter of the principal loci of activation for the group model. As in the group model, the average count data in a region, 5 by 5 by three voxels in the x, y and z dimensions, centered on the selected voxel — a volume of 1.2 cm^3 ($10 \times 10 \times 12$ mm) — for each subject.

Constructing the Single-subject Models

A correlation matrix was constructed for each individual based on the average intensity values derived from the subject's extracted 2-back regional activations — seven or 14 measures depending on how many repeat scans the subject had. Based on the group model, a WM model was constructed for each subject using that subject's interregional correlation matrix. The same nodes and paths in the group model were used to construct a model for each subject, with Ψ set to the value determined from the split-half test of the group model.

Testing the Single-subject Models

As for the group model, the stacked-model approach described above was used to test the goodness-of-fit of each single-subject against the group model. Path weights between individual nodes were then recorded for the alternative model for each of the single-subject models. Thus, the single-subject WM models differed from the group model only in terms of the values of each effective connection.

Exploring the Relationship Between Path Weights and Behavioral Measures

To establish the relationship between the recorded behavioral measures and the WM model, correlation analyses were conducted between path weights derived from individual models and performance and self-reported strategy scores. Prior to the correlational analyses all data were tested for normality of distribution using the Kolmogorov–Smirnov test.

Only models that met stability criteria established by AIC and RMSEA measures (Goncalves *et al.*, 2001) were used. Thus models from subjects who only had seven repeat scans were removed from the analysis because they were unstable — this left a total of 26 single-subject models. Self-reported strategy rating was collected from 14 of these remaining 26 subjects (six high-performers and eight low-performers — see below), who were entered into the correlation analysis of strategy with path weights.

Results

Behavioral Measures

The mean strategy score for the 14 subjects who reported it was 2.71 (SD = 1.4, range was 1–4.75). The 2-back performance score (percent correct) for each subject for each scan session was averaged to produce a single score per subject. The mean performance score for the 2-back task for the group of 26 subjects was 83% correct (SD = 14.3, range was 52.9% to 98.4%).

Examination of the performance scores' distribution suggested the existence of two groups: (i) high performers (HP, n = 16), with scores ranging from 84.7% to 98.4% (mean = 93.5, SD = 3.6), and (ii) low performers (LP, n = 10) with scores ranging from 52.9% to 75.6% (mean = 66.3, SD = 6.5), with the mean 2-back score significantly different between LP and HP groups [$t(24) = -13.7$, $P < 0.0005$]. There was no significant difference in age between groups [$t(24) = -0.61$, $P = 0.55$]. The male:female sex ratio for each group was HP = 12:4, LP = 3:7 ($\chi^2 = 3.72$, $P = 0.054$).

Voxel-based (SPM96) Statistical Activation Analysis

Figure 1 (right panel) shows the sites of increased activity in the SPM[Z] contrast of 2-back against 0-back conditions. Areas of increased activity were found bilaterally in the inferior parietal lobule (iPL), dorsolateral prefrontal cortex (dlPFC), thalamus (medial dorsal nucleus), cerebellum, left inferior frontal gyrus (Broca's area), and an extensive bilateral region of activation overlapping both the dorsal premotor areas (PMA) and anterior cingulate cortex (ACC) that made these regions indistinguishable (henceforth we refer to this as a single node labeled 'Cing'). There was a significant reduction in activity (not shown in the figure) in the 2-back compared with 0-back condition bilaterally in the parahippocampal gyrus (PHG).

Table 1 lists the regions activated, their Talairach coordinates, and the statistical results reported by SPM96. Most of the regions of activation have been reported in studies that use the *n*-back WM task with PET or fMRI (Cohen *et al.*, 1994; Smith and Jonides, 1998; Cabeza and Nyberg, 2000; Mottaghy *et al.*, 2000; Meyer-Lindenberg *et al.*, 2001), and some have been identified in monkey studies of WM (Rainer *et al.*, 1998; Chafee and Goldman-Rakic, 2000; Compte *et al.*, 2000).

Working Memory Group Model

The interregional correlation matrix for the 12 regions used in the SEM WM model is given in Table 2. Averaged data from all 39 subjects was used to build and test the model with the residual variance, Ψ, set to 0.7 for each node. There were a total of 19 paths, generally constructed to fit well with anatomical data prior to the modeling procedure. The path between the left and right iPL exists anatomically in primates (Clower *et al.*, 2001), as do the paths between the right and left parahippocampal regions, not shown in Figure 2 (Gloor *et al.*, 1993). The path between the medial dorsal nucleus of the left and right thalamus does not exist anatomically, but a strong functional connection was implied in the correlation analysis. We tested three models with different variants of this path: a single path from left to right thalamus; a single path, in the opposite direction (right to left); equally weighted bidirectional paths between the two thalami. The model that generated the best fit was for the path from the left to the right thalamus and this was the one included in the final model.

There was good fit for the group WM model [$\chi^2(59) = 71.3$, $P = 0.13$, AIC = –46.7, RMSEA = 0.07]. Goodness-of-fit using the χ^2 value is indicated when there is no significant difference between the observed and expected correlation matrices, as typified by a P-value > 0.1. Figure 2 shows the group model derived for the 2-back WM task. Among its prominent features were strong fronto-parietal effective connections on the left side of the brain and strong across-hemisphere effective connections between iPL regions. Strong effective connections between these regions were predicted as they are activated in reported WM neuroimaging studies.

Table 1

Principal sites of increases and decreases in activity for the SPM contrast of 2-back task versus the 0-back task listing the anatomical region of the maximum voxel intensity, its coordinates in Talairach space, the *Z*-value reported at that voxel and the corrected probability value taking account of multiple comparisons

Region	Brodmann area	Talairach coordinates	*Z*-value	*P*-value
Left dorsal PMA	6	–28 6 55	8.4	<0.0005
Right dorsal PMA	6	32 6 51	8.14	<0.0005
Left dlPFC	9/46	–46 29 28	8.18	<0.0005
Right dlPFC	9/46	42 30 24	8.86	<0.0005
Left iPL	40	–44 –41 43	8.54	<0.0005
Right iPL	40	44 –46 43	9.2	<0.0005
Left thalamus (MDN)		–10 15 12	6.82	0.012
Right thalamus (MDN)		10 –15 12	7.3	<0.0005
Anterior cingulate cortex	24/32	–2 16 40	8.65	<0.0005
Left PHG	27	–30 –24 –12	–7.9*	<0.0005
Right PHG	27	30 –22 –12	–7.38*	<0.0005
Right cerebellum		36 –54 –28	8.04	<0.0005
Left cerebellum		–36 –58 –27	8.75	<0.0005
Inf. frontal gyrus (Broca area)	44	44 8 11	4.62	0.056

Annotations: dlPFC = dorsolateral prefrontal cortex; PMA = premotor area; iPL = inferior parietal lobule; MDN = medial dorsal nucleus; PHG = parahippocampal gyrus. A procedure developed by Dr Matthew Brett (http://www.mrc-cbu.cam.ac.uk/Imaging/mnispace. html) was used to convert the MNI coordinates reported in SPM96 to Talairach coordinates and these are reported in the table.

The data were then spilt into two groups, matched for age, sex and performance and a split-half, stacked-model was tested while adjusting Ψ on the observed variables to get the lowest value possible with acceptable fit indices (AIC and RMSEA). Lowering the Ψ to 0.65 gave a χ^2_{diff} (19) = 27 ($P > 0.1$) between null and alternative models. The fit indices were good, AIC = –43.1 and RMSEA = 0.1. This determined the final group model with which to compare the individual, single-subject models.

Single-subject Models

The individual-subject correlation matrices were each fitted in turn to the group SEM model in MX. Thirty-nine stacked-models were then tested, as before with null and alternative models, but this time each individual subject's model was tested in turn against the group model, with all Ψ fixed at 0.65. All but two of the 13 models derived from subjects with seven repeat measures were inestimable, and one of those had an AIC > 0 with a large RMSEA. Thus it was decided to abandon the models from subjects with seven repeat scans only. This left a group of 26 models representing the 26 remaining subjects, comprising 11 females and 15 males, mean age 30 (range 20–48), and all of these models were stable, as indicated by the AIC and RMSEA goodness-of-fit indices.

Seven of the 26 individual models had a $\chi^2_{diff} < \chi^2_{critcal}$ giving a P-value > 0.1. In other words those subjects had path models that resembled the group model in terms of the path weights between nodes. Four of these subjects were from the HP group, three from the LP group and only four reported their strategy: one mainly spatial, the rest split between verbal and spatial. The remainder of the models varied, consistent with the notion of individual differences in network activity (Goncalves *et al.*, 2001), and indicating sufficient variability to support the correlational analyses below.

t-tests Across HP and LP Groups: Performance Scores and Path Weights

t-tests were then performed across the two separate HP and LP groups' SEM WM path weights. Two paths significantly differed between the HP and LP groups: left iPL – right PHG ($t(24) = 2.21$, $P = 0.037$: $LP_{mean} = 0.15$, SD = 0.29; $HP_{mean} = -0.14$, SD = 0.34) and right iPL – left PHG [$t(24) = 2.203$, $P = 0.037$: $LP_{mean} = 0.112$, SD = 0.308; and $HP_{mean} = -0.127$, SD = 0.245]. Note that

Table 2

The matrix was derived from the average of all scans for each subject for the 2-back task

	BROCA	LPHG	LCEREB	LDLPFC	LIPL	LTHAL	RPHG	RCEREB	RDLPFC	RIPL	RTHAL	CING
BROCA	1											
LPHG	0.051	1										
LCEREB	0.065	–0.055	1									
LDLPFC	0.111	0.052	–0.024	1								
LIPL	0.643	0.083	–0.051	0.149	1							
LTHAL	–0.066	0.027	0.322	–0.204	–0.326	1						
RPHG	–0.170	0.344	0.033	0.011	–0.169	0.141	1					
RCEREB	0.205	–0.294	0.447	–0.337	0.102	0.244	–0.148	1				
RDLPFC	0.177	–0.078	0.198	–0.123	0.232	0.111	0.049	0.328	1			
RIPL	0.331	–0.175	0.294	0.011	0.551	–0.077	–0.106	0.317	0.104	1		
RTHAL	–0.13	–0.058	–0.04	–0.28	–0.321	0.591	–0.134	0.138	–0.201	–0.110	1	
CING	0.045	0.027	0.051	0.123	–0.061	0.049	–0.126	–0.073	0.278	–0.148	–0.059	1

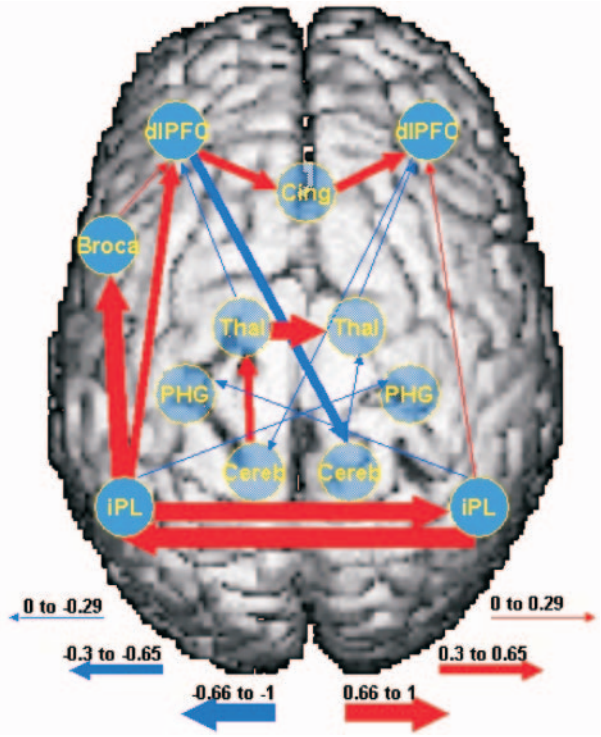

Figure 2. Group path model. Positively weighted paths are colored red, negatively weighted paths are colored blue. Thicker arrows indicate stronger connections. Two paths — from right PHG to left PHG and left PHG to right PHG — have been omitted for clarity. The strengths of both these paths was +0.7. Annotations: PHG = parahippocampal gyrus; dlPFC = dorsolateral prefrontal cortex; Cing = cingulate cortex; iPL = inferior parietal lobule; Thal = thalamus; Cereb = cerebellum; Broca = Broca's area.

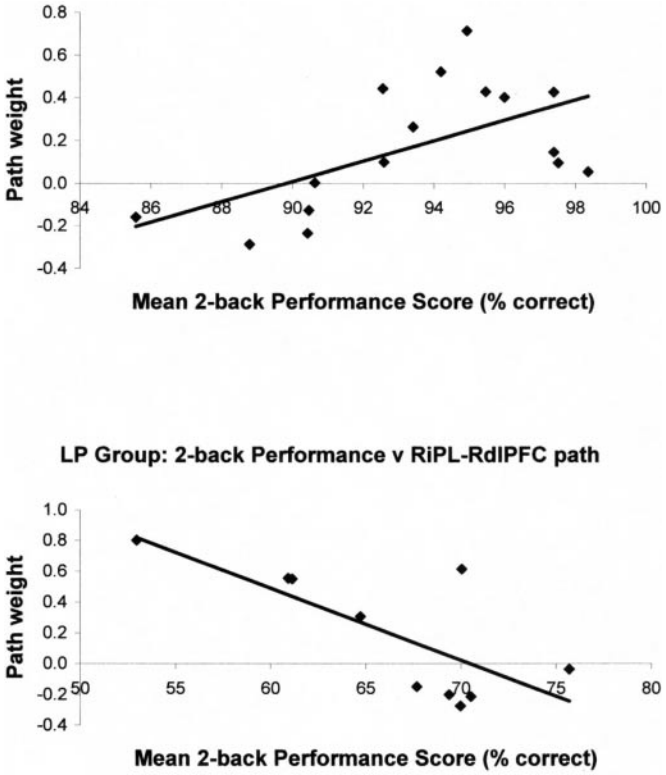

Figure 3. Upper: correlation of 2-back performance score (percent correct) against the path weight between LiPL and Broca's region in the high-performance group (n = 16, r = 0.584, P = 0.018). Lower: correlation of 2-back performance score (per cent correct) against the path weight between RiPL and RdlPFC in the low-performance group (n = 12, r = –0.737, P = 0.015).

the iPL to contralateral PHG paths are negative in the HP group and positive in the LP group. Because there was a trend for a sex-ratio difference between the LP and HP groups, the original group of 26 subjects was split into two groups by sex (11 females, 15 males) and the t-test analysis above repeated. This time, only 2-back performance score was significantly different (t = –2.84, P = 0.009: female mean = 74.4 (SD = 13.5); male mean = 89.6 (SD = 11.8)), with left iPL – right PHG path (p = 0.86) and iPL – left PHG (p = 0.5) now failing to show statistically significant differences. Thus, this result suggests that group differences in path weights are related mainly to performance, not sex, although the influence of sex cannot be completely ruled out.

Task Performance Correlations

In the first set of correlation analyses the subjects' path weights were correlated against the 2-back performance scores separately for each group. For the HP group, there was a significant positive correlation between the left iPL – Broca path (r = 0.584, P = 0.018; for the LP group, this correlation was r = 0.07, P = 0.854). For the LP group, there was a significant negative correlation for the right iPL – right DLPFC path (r = –0.737, P = 0.015; for the HP group, this correlation was r = 0.021, P = 0.937). The significant results are shown in Figure 3.

A correlation analysis of path weights against 2-back performance score was performed for the combined group of subjects. There were two results of note, both of borderline statistical significance: the left iPL – right PHG path (r = –0.383, P = 0.054) and the right iPL – left PHG path (r = –0.374, P = 0.06).

Task Strategy Correlations

Next, a correlation analysis was performed between path weights and the self-reported strategy scores for the 14 subjects (six LP, eight HP) for whom strategy data were collected. There was a significant correlation showing increasing spatial strategy with the left iPL – right PHG path strength (r = 0.66, P = 0.01, Fig. 4). A correlation analysis was then carried out for each group, showing that strategy correlated positively with the path between left iPL – right PHG in the HP group only (r = 0.755, P = 0.03). The strategy scores for the two groups, while not significantly different [HP_{mean} = 2.2 (SD = 1.2); LP_{mean} = 3.3 (SD = 1.02)], showed a trend for the HP group to use a verbal strategy with 6/8 subjects having a score less than three. In contrast, no LP subjects showed a distinctly verbal strategy.

Discussion

Using SEM, we have produced a group average functional network model for the 2-back WM task. This model prominently involved strong functional links between parietal and frontal cortex. Moreover, embedded in this group average network were two distinct brain sub-networks that, when viewed for individual subjects, appear uniquely associated with a subject's innate ability to perform the task. Subjects who performed the task most successfully utilized a left hemisphere

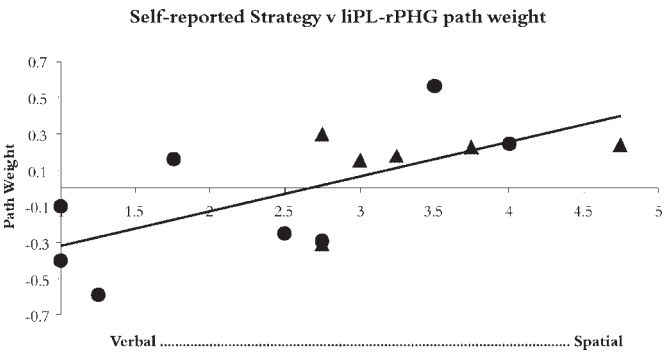

Figure 4. The correlation of strategy and path weight for the left inferior parietal lobule and the right parahippocampal gyrus. Circles denote subjects in the HP group; triangles denote subjects in the LP group. There was no correlation with path weight and strategy for the LP group; for the HP group $r = 0.755$, $P = 0.03$; for the combined group, $r = 0.66$, $P = 0.01$ for all subjects who reported their strategy ($n = 14$).

network involving the iPL and Broca areas whereas subjects who performed less well employed a right hemisphere network involving the iPL and dlPFC. While the importance of the frontal–parietal association in individual cognitive characteristics was predicted, the results extend our predictions by providing new information about the neural mechanisms mediating these performance differences. We have also shown that self-reported strategy is reflected at the cortical level, specifically in a sub-network involving an effective connection between the PHG and iPL. An intriguing association between strategy and performance level was observed in this same sub-network.

The Group Average WM Model

The model constructed from the group average activity is consistent with many functional neuroimaging activation studies of WM. In such studies the regions that consistently activate are frontal, parietal, cingulate and cerebellum. We observed strong effective connections involving all these regions, especially fronto-parietal and inter-parietal links.

The dlPFC and iPL regions are heavily interconnected in primates (Cavada and Goldman-Rakic, 1989) and it has been shown these regions subserve WM processes in both single neuron primate recordings and human neuroimaging studies. Neurons in these regions behaved interdependently during a WM task in primates (Chafee and Goldman-Rakic, 2000). WM load-dependent activity has been seen in posterior parietal cortex (Honey *et al.*, 2000) and prefrontal cortex (Manoach *et al.*, 1997) and collaborative activity is implied in WM from human neuroimaging (Diwadkar *et al.*, 2000; Mottaghy *et al.*, 2000; Bokde *et al.*, 2001), EEG (Chao and Knight, 1996; Gevins and Smith, 2000; Ross and Segalowitz, 2000) and TMS (Muri *et al.*, 2000; Oliveri *et al.*, 2001) studies. It has been suggested that the iPL serves as a phonological maintenance or short-term storage area (Paulesu *et al.*, 1993; Jonides *et al.*, 1998; Smith and Jonides, 1998), although other studies find a load-dependent activation (Callicott *et al.*, 1999; Jansma *et al.*, 2000) that might reflect other concurrent processes such as encoding and retrieval, or that the iPL may have a role in the processing of specialized visual information (Ungerleider *et al.*, 1998). The dlPFC is thought to be associated with planning, monitoring and response selection in primates (Levy and Goldman-Rakic, 2000; Petrides, 2000) and, additionally, in human neuroimaging studies, with all phases of encoding, maintenance, retrieval (Braver *et al.*, 1997; Cohen *et al.*, 1997; Cabeza and Nyberg, 2000) and manipulation (D'Esposito *et al.*, 1999).

It is interesting that the strongest group average fronto-parietal effective connections were in the left hemisphere. As in all group average data the characteristics of the individuals comprising the group may be obscured, particularly if these individuals employ diverse strategies and/or have differences in innate ability, as was demonstrated in our behavioral data. Our single-subject analyses, to which we now turn, help elucidate this.

Single-subject SEM Models

We observed considerable interindividual variability in single-subject models and in individual path weights, as has been reported in a few other SEM studies (e.g. Goncalves *et al.*, 2001). Our results suggest that this type of neurobiological variability has implications for, and reflects, differences in cognitive style and ability during WM.

Fronto-parietal Connectivity and WM Performance As a Function of Hemisphere

Not only do our findings confirm that there is strong bilateral collaborative activity between frontal and parietal regions in the 2-back task, they also indicate that the degree of fronto-parietal coupling within each hemisphere appears to reflect performance level in individual subjects. Specifically, in the HP group performance scores increased as the iPL-Broca's area path-strength on the left increased (Fig. 3, upper) and in LP group the iPL-dlPFC path-strength in the right hemisphere became weaker as performance scores improved (Fig. 3, lower). Although the exact nature of these relationships was not predicted, our results are consistent with and expand upon published findings that lead to our hypothesis linking frontal–parietal interactions and WM performance. It has been proposed that a right fronto-parietal network is activated for sustained attention, and a left fronto-parietal network for the phonological rehearsal loop component of WM (Coull *et al.*, 1996). However, the same authors suggest that activation of the right hemisphere network may also indicate that subjects are activating a visuospatial buffer (Baddeley, 1992), putatively in the right inferior parietal lobule. EEG activity has also been found to be more prevalent in the left hemisphere of subjects of high verbal ability, while predominantly right-sided EEG activity is present in subjects with more spatial ability (Gevins and Smith, 2000). In general, verbal/numeric WM tasks appear to activate a network in the left hemisphere while spatial WM tasks appear to activate a right hemispheric network, although this pattern is by no means unequivocal in every study or in every individual subject in our present study, and bilateral activity often occurs in both types of tasks (Cabeza and Nyberg, 2000). In our study, subjects who performed poorly appeared to activate a right hemisphere fronto-parietal connection whilst subjects who performed well favored a similar, but left-sided, network. Possible explanations for this may be related to either innate cognitive ability and/or to the strategy that the subjects use to perform the task.

It is possible that the predominance of the left-hemisphere fronto-parietal connectivity in the group model reflects the fact that there were more high performers in the study, and they used a left-sided network. This demonstrates the power that the

single-subject SEM approach has for resolving the individual contributions hidden within the group average model.

Parietal–Hippocampal Connectivity and WM Strategy

The number of subjects for whom we had strategy data was small, and we did not have an *a priori* hypothesis regarding this interaction, thus we may attach only limited significance to the results. However, the relationship between WM strategy and iPL-contralateral PHG path strength is intriguing. As shown in Figure 4, (i) there was a positive correlation between path weight and strategy across all subjects; (ii) the HP group tended to have a verbal strategy and a positive correlation with path weight and (iii) there was no correlation of strategy with path coefficient in the LP group. The LP subjects are grouped towards the middle and the spatial end of the verbal:spatial continuum, the HP subjects mainly to the verbal end.

There is anatomical support for the presence of a parietal-hippocampal functional link. Within the medial temporal lobe, the hippocampus is heavily connected to the adjacent perirhinal and entorhinal cortices, and left and right hippocampii are interconnected via the fornix (Gloor *et al.*, 1993) and also to both ipsilateral and contralateral iPL (Clower *et al.*, 2001) in primates. The PHG receives cortical inputs from posterior parietal cortex (Lavenex and Amaral, 2000), and, like the hippocampus, has not been associated with WM but with declarative long-term memory (LTM) formation (Lavenex and Amaral, 2000). However, recent neuroimaging studies have shown that the hippocampus and PHG may be involved in WM processes. In a task using novel and learned faces, a clear dissociation of function was demonstrated between anterior hippocampus and PHG, with the former being active during WM delay and the latter activating during both WM and LTM encoding and retrieval (Ranganath and D'Esposito, 2001). A study using spatial alternation with a WM maintenance demand showed activation in the right hippocampus during alternation (Curtis *et al.*, 2000).

The role of the iPL as a WM buffer was outlined above and it has been suggested that hippocampal–parietal interaction is present in the process of spatial cognition (Maguire *et al.*, 1998; Save and Poucet, 2000). Our study showed that subjects who utilize a more self-reported spatial strategy have a positively weighted connection between left iPL and right PHG, while those claiming a more verbal strategy have a negatively weighted connection. Understanding the neural substrate of SEM path weight polarity (positive or negative) is necessary to make inferences on our results. Path weights are essentially linear regression coefficients with the sign implying the positive or negative influence of one node on another. The magnitude of the weight gives the strength of the regression. It has been suggested that relative suppression of activity at one node with respect to another produces path weights that are negative, implying that this represents an inhibitory process at the neuronal level (Nyberg *et al.*, 1996), although it is also possible that a third area not included in the model exerts this influence. This possibility was not explicitly tested in our study, but if we assume subjects using a verbal strategy exhibit a suppression of neuronal activity in the iPL–PHG connection, we speculate that the process is suppressing the formation of LTM. Spatial strategists, who tend to perform worse, appear to activate this connection, which may, in turn, imply activation of an LTM process, such as encoding, that is not advantageous for this WM task.

Single-subject Studies Using SEM

It has been suggested that the number of subjects or number of repeat measures required to construct a stable SEM model should either be large or the effect size should be large and normally distributed in smaller groups (Ullman, 1996), with a minimum of 10 subjects. Our study has confirmed that, for individual subjects, the number of repeat-measures required to create a stable model with methods similar to ours is greater than seven, because most models using only seven repeat-measures were inestimable.

Of the 26 single-subject models produced, seven had path weights closely representing those of the group average model. Because the goodness-of-fit measures are applied to the entire network, rather than individual paths, it is possible for the strengths and polarities of individual paths to vary considerably, even across individuals who have models with very similar fit indices. This emphasizes the interindividual variability of the network as a whole, and shows that SEM can capture this individual variability and model complex brain networks to reveal how these networks are utilized in different individuals.

Conclusions

Using SEM, a group WM model is described that shows prominent effective connections particularly on the left side of the brain. Analyses of single-subject SEM WM models revealed underlying cortical sub-networks in each hemisphere that are related to behavioral measures. The performance and strategy analyses indicated that subjects who utilized a verbal strategy perform our 2-back WM task more efficiently than those who utilized a spatial strategy. This point is supported by the fact that the LP group tended to use a more equally mixed verbal:spatial or mainly spatial strategy, whereas the HP group tended to use a mainly verbal strategy (6/8 subjects). The path analysis suggests that suppression of LTM may be a more efficient use of neuronal resources than activation of LTM in this WM task. It is also conceivable that the task is easier to perform using a verbal rather than a spatial strategy, where use of subvocal rehearsal of the numbers is more effective than remembering their spatial position. Differences in performance could then be due to either differences in innate cognitive ability or because some subjects make a decision — consciously or subconsciously — on a strategy that is either optimally matched, or not optimally matched to the task. This may have important implications in the study of mental illness, such as schizophrenia, where subjects are known to perform WM tasks poorly (Manoach *et al.*, 1999, 2000; Callicott *et al.*, 2000; Meyer-Lindenberg *et al.*, 2001). Despite innate capacity limitations (Goldberg *et al.*, 1998; Callicott *et al.*, 2000) or aberrant dopaminergic function (Meyer-Lindenberg *et al.*, 2002), it is possible that assistance with selecting a more rewarding strategy might improve the performance of these subjects and could form the basis of a future study.

Notes

We thank Dr Michael Neale of the Virginia Commonwealth Institute for useful discussions on the application of his MX software to our data. The invaluable help of Dr Daniel R Weinberger, Clinical Brain Disorders Branch, NIMH, in reviewing the manuscript is also acknowledged.

Address correspondence to Michael F. Glabus, Ph.D., Department of Psychiatry, Louisiana State University Health Sciences Center, PO Box, 33932, 1501 Kings Highway, Shreveport, LA 71130-3932, USA. Email: mglabu@lsuhsc.edu.

References

Akaike AC (1987) Factor analysis and AIC. Psychometrika 52:317–332.

Andreasen NC, Paradiso S,O'Leary DS (1998) 'Cognitive dysmetria' as an integrative theory of schizophrenia: a dysfunction in cortical–subcortical–cerebellar circuitry? Schizophr Bull 24:203–218.

Baddeley A (1992) Working memory. Science 255:556–559.

Bokde AL, Tagamets MA, Friedman RB, Horwitz B (2001) Functional interactions of the inferior frontal cortex during the processing of words and word-like stimuli. Neuron 30:609–617.

Braver TS, Cohen JD, Nystrom LE, Jonides J, Smith EE, Noll DC (1997) A parametric study of prefrontal cortex involvement in human working memory. Neuroimage 5:49–62.

Browne M, Cudeck R (1993) Alternative ways of assessing model fit. In: Testing structural equation models (Bollen KA, Long JS, eds), pp. 132–162. Beverley Hills, CA: Sage.

Buchel C, Friston KJ (1997) Modulation of connectivity in visual pathways by attention: cortical interactions evaluated with structural equation modelling and fMRI., Cereb Cortex 7:768–778.

Buchel C, Coull JT, Friston KJ (1999) The predictive value of changes in effective connectivity for human learning. Science 283:1538–1541.

Bullmore E, Horwitz B, Honey G, Brammer M, Williams S, Sharma T (2000) How good is good enough in path analysis of fMRI data? Neuroimage 11:289–301.

Cabeza R, Nyberg L (2000) Imaging cognition II: An empirical review of 275 PET and fMRI studies. J Cogn Neurosci 12:1–47.

Callicott JH, Ramsey NF, Tallent K, Bertolino A, Knable MB, Coppola R, Goldberg T, van Gelderen P, Mattay VS, Frank JA, Moonen CT, Weinberger DR (1998) Functional magnetic resonance imaging brain mapping in psychiatry: methodological issues illustrated in a study of working memory in schizophrenia. Neuropsychopharmacology 18:186–196.

Callicott JH, Mattay VS, Bertolino A, Finn K, Coppola R, Frank JA, Goldberg TE, Weinberger DR (1999) Physiological characteristics of capacity constraints in working memory as revealed by functional MRI., Cereb Cortex 9:20–26.

Callicott JH, Bertolino A, Mattay VS, Langheim FJ, Duyn J, Coppola R, Goldberg TE, Weinberger DR (2000) Physiological dysfunction of the dorsolateral prefrontal cortex in schizophrenia revisited. Cereb Cortex 10:1078–1092.

Cavada C, Goldman-Rakic PS (1989) Posterior parietal cortex in rhesus monkey: II., Evidence for segregated corticocortical networks linking sensory and limbic areas with the frontal lobe. J Comp Neurol 287:422–445.

Chafee MV, Goldman-Rakic PS (1998) Matching patterns of activity in primate prefrontal area 8a and parietal area 7ip neurons during a spatial working memory task. J Neurophysiol 79:2919–2940.

Chafee MV, Goldman-Rakic PS (2000) Inactivation of parietal and prefrontal cortex reveals interdependence of neural activity during memory-guided saccades. J Neurophysiol 83:1550–1566.

Chao LL, Knight RT (1996) Prefrontal and posterior cortical activation during auditory working memory. Brain Res Cogn Brain Res 4:27–37.

Clower DM, West RA, Lynch JC, Strick PL (2001) The inferior parietal lobule is the target of output from the superior colliculus, hippocampus, and cerebellum. J Neurosci 21:6283–6291.

Cohen JD, Forman SD, Braver TS, Casey BJ, Servan-Schreiber D, Noll DC (1994) Activation of prefrontal cortex in a nonspatial working memory task with functional MRI. Hum Brain Mapp 1:293–304.

Cohen JD, Perlstein WM, Braver TS, Nystrom LE, Noll DC, Jonides J, Smith EE (1997) Temporal dynamics of brain activation during a working memory task. Nature 386:604–608.

Compte A, Brunel N, Goldman-Rakic PS, Wang XJ (2000) Synaptic mechanisms and network dynamics underlying spatial working memory in a cortical network model. Cereb Cortex 10:910–923.

Coull JT, Frith CD, Frackowiak RS, Grasby PM (1996) A fronto-parietal network for rapid visual information processing: a PET study of sustained attention and working memory. Neuropsychologia 34:1085–1095.

Curtis CE, Zald DH, Lee JT, Pardo JV (2000) Object and spatial alternation tasks with minimal delays activate the right anterior hippocampus proper in humans. Neuroreport 11:2203–2207.

D'Esposito M, Postle BR, Ballard D, Lease J (1999) Maintenance versus manipulation of information held in working memory: an event-related fMRI study. Brain Cogn 41:66–86.

Diwadkar VA, Carpenter PA, Just MA (2000) Collaborative activity between parietal and dorso-lateral prefrontal cortex in dynamic spatial working memory revealed by fMRI., Neuroimage 12:85–99.

Friedman HR, Goldman-Rakic PS (1994) Coactivation of prefrontal cortex and inferior parietal cortex in working memory tasks revealed by 2DG functional mapping in the rhesus monkey. J Neurosci 14:2775–2788.

Friston K (1994) Functional and effective connectivity in neuroimaging: a synthesis. Hum Brain Mapp 2:56–78.

Friston K, Holmes A, Worsley K, Poine J-B, Frith C, Frackowiak R (1995) Statistical parametric maps in functional imaging: a general linear approach. Hum Brain Mapp 2:189–210.

Gevins A, Cutillo B (1993) Spatiotemporal dynamics of component processes in human working memory. Electroencephalogr Clin Neurophysiol 87:128–143.

Gevins, A and Smith, ME (2000) Neurophysiological measures of working memory and individual differences in cognitive ability and cognitive style. Cereb Cortex 10:829–839.

Gloor P, Salanova V, Olivier A, Quesney LF (1993) The human dorsal hippocampal commissure. An anatomically identifiable and functional pathway. Brain 116:1249–1273.

Goldberg TE, Patterson KJ, Taqqu Y, Wilder K (1998) Capacity limitations in short-term memory in schizophrenia: tests of competing hypotheses. Psychol Med 28:665–673.

Goncalves MS, Hall DA, Johnsrude IS, Haggard MP (2001) Can meaningful effective connectivities be obtained between auditory cortical regions? Neuroimage 14:1353–1360.

Hartley AA, Speer NK (2000) Locating and fractionating working memory using functional neuroimaging: storage, maintenance, and executive functions. Microsc Res Tech 51:45–53.

Honey GD, Bullmore ET, Sharma T (2000) Prolonged reaction time to a verbal working memory task predicts increased power of posterior parietal cortical activation. Neuroimage 12:495–503.

Horwitz B, McIntosh AR, Haxby JV, Furey M, Salerno JA, Schapiro MB, Rapoport SI, Grady CL (1995) Network analysis of PET-mapped visual pathways in Alzheimer type dementia. Neuroreport 6:2287–2292.

Horwitz B, Tagamets M-A, McIntosh AR (1999) Neural modeling, functional brain imaging and cognition. Trends Cogn Sci 3:91–98.

Jansma JM, Ramsey NF, Coppola R, Kahn RS (2000) Specific versus nonspecific brain activity in a parametric N-back task. Neuroimage 12:688–697.

Jonides J, Schumacher EH, Smith EE, Koeppe RA, Awh E, Reuter-Lorenz PA, Marshuetz C, Willis CR (1998) The role of parietal cortex in verbal working memory. J Neurosci 18:5026–5034.

Kim SG, Ugurbil K, Strick PL (1994) Activation of a cerebellar output nucleus during cognitive processing. Science 265:949–951.

Lavenex P, Amaral DG (2000) Hippocampal–neocortical interaction: a hierarchy of associativity. Hippocampus 10:420–430.

Levy R, Goldman-Rakic PS (2000) Segregation of working memory functions within the dorsolateral prefrontal cortex. Exp Brain Res 133:23–32.

Logothetis NK, Pauls J, Augath M, Trinath T, Oeltermann A (2001) Neurophysiological investigation of the basis of the fMRI signal. Nature 412:150–157.

Maguire EA, Burgess N, Donnett JG, Frackowiak RS, Frith CD,O'Keefe J (1998) Knowing where and getting there: a human navigation network. Science 280:921–924.

Manoach DS, Schlaug G, Siewert B, Darby DG, Bly BM, Benfield A, Edelman RR, Warach S (1997) Prefrontal cortex fMRI signal changes are correlated with working memory load. Neuroreport 8:545–549.

Manoach DS, Press DZ, Thangaraj V, Searl MM, Goff DC, Halpern E, Saper CB, Warach S (1999) Schizophrenic subjects activate dorsolateral prefrontal cortex during a working memory task, as measured by fMRI., Biol Psychiatry 45:1128–1137.

Manoach DS, Gollub RL, Benson ES, Searl MM, Goff DC, Halpern E, Saper CB, Rauch SL (2000) Schizophrenic subjects show aberrant fMRI acti-

vation of dorsolateral prefrontal cortex and basal ganglia during working memory performance. Biol Psychiatry 48:99–109.
McIntosh A, Gonzalez-Lima F (1994) Structural equation modeling and its application to network analysis in functional brain imaging. Hum Brain Mapp 2:2–22.
McIntosh AR, Grady CL, Haxby JV, Ungerleider LG, Horwitz B (1996a) Changes in limbic and prefrontal functional interactions in a working memory task for faces. Cereb Cortex 6:571–584.
McIntosh AR, Bookstein FL, Haxby JV, Grady CL., (1996b) Spatial pattern analysis of functional brain images using partial least squares. Neuroimage 3:143–157.
Meyer-Lindenberg A, Poline JB, Kohn PD, Holt JL, Egan MF, Weinberger DR, Berman KF (2001) Evidence for abnormal cortical functional connectivity during working memory in schizophrenia. Am J Psychiatry 158:1809–1817.
Meyer-Lindenberg A, Miletich RS, Kohn PD, Esposito G, Carson RE, Quarantelli M, Weinberger DR, Berman KF (2002) Reduced prefrontal activity predicts exaggerated striatal dopaminergic function in schizophrenia. Nat Neurosci 5:267–271.
Middleton FA, Strick PL (1994) Anatomical evidence for cerebellar and basal ganglia involvement in higher cognitive function. Science 266:458–461.
Middleton FA, Strick PL (2000) Basal ganglia and cerebellar loops: motor and cognitive circuits. Brain Res Brain Res Rev 31:236–250.
Middleton FA, Strick PL (2001) Cerebellar projections to the prefrontal cortex of the primate. J Neurosci 21:700–712.
Mottaghy FM, Krause BJ, Kemna LJ, Topper R, Tellmann L, Beu M, Pascual-Leone A, Muller-Gartner HW (2000) Modulation of the neuronal circuitry subserving working memory in healthy human subjects by repetitive transcranial magnetic stimulation. Neurosci Lett 280:167–170.
Muri RM, Gaymard B, Rivaud S, Vermersch A, Hess CW, Pierrot-Deseilligny C (2000) Hemispheric asymmetry in cortical control of memory-guided saccades. A transcranial magnetic stimulation study. Neuropsychologia 38:1105–1111.
Neale M, Boker S, Xie G, Maes H (1999) MX: Statistical modelling. Richmond, VA: Virginia Commonwealth University.
Nyberg L, McIntosh AR, Cabeza R, Nilsson LG, Houle S, Habib R, Tulving E (1996) Network analysis of positron emission tomography regional cerebral blood flow data: ensemble inhibition during episodic memory retrieval. J Neurosci 16:3753–3759.
Oliveri M, Turriziani P, Carlesimo GA, Koch G, Tomaiuolo F, Panella M, Caltagirone C (2001) Parieto-frontal interactions in visual-object and visual-spatial working memory: evidence from transcranial magnetic stimulation. Cereb Cortex 11:606–618.
Paulesu E, Frith CD, Frackowiak RS (1993) The neural correlates of working memory. Nature 362:342–345.
Petrides M (2000) The role of the mid-dorsolateral prefrontal cortex in working memory. Exp Brain Res 133:44–54.
Petrides M, Pandya DN (1999) Dorsolateral prefrontal cortex: comparative cytoarchitectonic analysis in the human and the macaque brain and corticocortical connection patterns. Eur J Neurosci 11:1011–1036.
Rainer G, Asaad WF, Miller EK (1998) Selective representation of relevant information by neurons in the primate prefrontal cortex. Nature 393:577–579.
Ranganath C, D'Esposito M (2001) Medial temporal lobe activity associated with active maintenance of novel information. Neuron 31:865–873.
Ross P, Segalowitz SJ (2000) An EEG coherence test of the frontal dorsal versus ventral hypothesis in N-back working memory. Brain Cogn 43:375–379.
Rypma B, D'Esposito M (1999) The roles of prefrontal brain regions in components of working memory: effects of memory load and individual differences. Proc Natl Acad Sci USA 96:6558–6563.
Save E, Poucet B (2000) Hippocampal–parietal cortical interactions in spatial cognition. Hippocampus 10:491–499.
Smith EE, Jonides J (1998) Neuroimaging analyses of human working memory. Proc Natl Acad Sci USA 95:12061–12068.
Smith EE, Jonides J (1999) Storage and executive processes in the frontal lobes. Science 283:1657–1661.
Ullman J (1996) Structural equation modeling: In: Using multivariate statistics (Tabachnick G, Fidell L, eds), pp. 709–811. New York: Harper Collins.
Ungerleider LG, Courtney SM, Haxby JV (1998) A neural system for human visual working memory. Proc Natl Acad Sci USA 95:883–890.
Waldvogel D, van Gelderen P, Muellbacher W, Ziemann U, Immisch I, Hallett M (2000) The relative metabolic demand of inhibition and excitation. Nature 406:995–998.
Weinberger D, Mattay V, Callicott J, Kotrla K, Santha A, van Gelderen P, Duyn J, Moonen C, Frank J (1996) fMRI applications in schizophrenia research. Neuroimage 4:118–126.
Woods RP, Cherry SR, Mazziotta SR (1992) Rapid automated algorithm for aligning and reslicing PET images. J Comput Assist Tomogr 16:620–633.